Snake's Perspective on Heat: Reconstruction of Input Using an Imperfect Detection System

Andreas B. Sichert, Paul Friedel, and J. Leo van Hemmen

Physik Department, Technische Universität München, 85747 Garching bei München, Germany
(Received 30 March 2006; published 9 August 2006)

Two groups of snakes possess an infrared detection system that is used to create a heat image of their environment. In this Letter we present an explicit reconstruction model, the ''virtual lens,'' which explains how a snake can overcome the optical limitations of a wide aperture pinhole camera, and how ensuing properties of the receptive fields on the infrared-sensitive membrane may explain the behavioral performance of this sensory system. Our model explores the optical quality of the infrared system by detailing how a functional representation of the thermal properties of the environment can be created. The model is easy to implement neuronally and agrees well with available neuronal, physiological, and behavioral data on the snake infrared system.

Two groups of snakes, pit vipers and boids, possess a sensory system to detect infrared (ir) radiation [1] which allows them to perceive a 2-dimensional image of the heat distribution in their surroundings. The detection system consists of a set of cavities called pit organs. In pit vipers, a pit organ is located on each side of the snake's head near the eyes. Suspended in each cavity is a heat detecting membrane, which is sensitive to mK temperature differences [2,3]. The optical principle underlying the detection of ir radiation is that of a pinhole camera (Fig. 1). Radiation entering through the pit hole hits the membrane at a certain spot depending on the source direction. The resulting temperature change at this spot is detected by heat-sensitive cells distributed throughout the membrane. There are about 40×40 sensory cells on the membrane [1] and the field of view is about 100° wide, which implies that input to the organ could be represented in the brain with a resolution of approximately 2.5°. Since the radiation flux entering the organ must be large enough to quickly detect moving prey, the aperture of the organ is wide, approximately 1 mm, and comparable to the organ depth. Thus incoming radiation from a point source does not strike a pointlike region on the membrane, as in an ideal pinhole camera, but rather a large disc-shaped region [Fig. 1(b)]. It is nonetheless possible to determine the direction of the incoming radiation if the boundary of the disc-shaped region remains narrow enough. This approach breaks down if multiple or non-pointlike heat sources (as in Fig. 2) are present. Then the resulting heat distribution on the membrane will be heavily blurred (see Fig. 3, left), allowing no direct evaluation of the input.

The ir detection system of snakes presents a paradox. The optics of the pit organ as pinhole camera ensure that images on the membrane will be distended and blurry. Yet the information from the ir system, combined with input from the ''normal'' visual system, allows formation of a *neuronal map* [4] in the brain's *optic tectum* [5–7]. This map is sharp enough to serve as a *topological* representation of the outside world, in that neighboring neurons

represent neighboring regions of the outside world. Experimental studies have shown that a snake's orientation to a point source of heat varies, but that an accuracy of 5° is nevertheless attainable [5], which approximates our rough estimate above. We are thus faced with a paradox, in that the optical quality of a pit organ is low but the neuronal performance is high. How does that happen?

The paradox involves the optical quality of ir ''vision.'' We therefore explore this optical quality by presenting an explicit model which reconstructs the original heat distribution in space using *only* the given heat distribution on the membrane. Our model can be implemented straightforwardly as a neuronal network. Furthermore, it explains several experimentally determined characteristics of ir detection in snakes.

The mathematical model describing the ir system consists of two parts. We first calculate the heat distribution on the membrane for a given heat distribution in space. Starting from this membrane image, the second step is reconstructing the original spatial heat distribution. We develop a *virtual lens* which replaces the oversized pin-
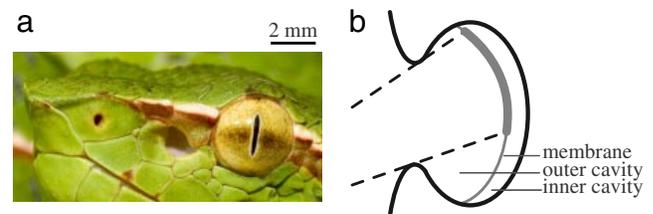

FIG. 1 (color online). (a) Head of a pit viper with nostril, (large) pit hole, and eye, left to right. Photograph courtesy of Guido Westhoff. (b) A pit viper's infrared-sensitive pit organ works like a pinhole camera. Radiation entering through the opening (left) hits a heat-sensitive membrane, suspended freely so as to minimize heat loss to the surrounding tissue. To ensure a large enough energy influx, the aperture has to be quite large (∼ 1 mm). The image of a pointlike source thus forms a disc-shaped image on the membrane.

hole. Since a snake has limited computational resources (all "calculations" must be realizable in neuronal "hardware") the reconstruction model must be simple. Our model thus uses only one computational step (it is *noniterative*) to estimate the input image from the measured response on the pit membrane. It resembles a Wiener filter and is akin to, but different from, some of the algorithms used in image reconstruction [8]. It has to be constantly borne in mind that the optical device discussed here has *very* limited imaging capabilities in comparison to human-devised detection systems; cf. Figure 1(b). Nonetheless, as we will show, it is still capable of reconstructing the spatial heat distribution.

The input to a pit organ consists of a 3-dimensional spatial heat distribution. To strike his prey, the snake needs a 2-dimensional projection, or image, of this heat distribution. This image is reconstructed using the response from the ir receptors on the pit membrane. Calling the true projection of the heat distribution I_α, we write the heat intensity S_α as it is measured by the sensory cells in the pit membrane

$$S_\alpha = T_\alpha{}^\beta (I_\beta + \psi_\beta) + \chi_\alpha. \qquad (1)$$

Here we use tensor notation and imply summation over repeated upper and lower indices. Simultaneous raising and lowering the indices of a tensor is equivalent to transposition in matrix notation. The tensor $T_\alpha{}^\beta$ is the transfer matrix (containing the point-response functions) that relates input intensity at the spatial location β to intensity at the membrane location α. It is determined solely by the *geometry* of the pit organ. ψ_β and χ_α are stochastic terms taking into account noise in the input signal and measurement errors, respectively.

In snake ir reception α and β represent the two spatial dimensions of the input image and the pit membrane surface. We represent the reconstruction $\hat{I}_\alpha$ of the input I_α as a *linear* combination of the measured intensities,

$$\hat{I}_\alpha = R_\alpha{}^\beta S_\beta. \qquad (2)$$

To find the coefficients of the reconstruction tensor $R_\alpha{}^\beta$ we define the quadratic error of our estimate (2) as

$$E_q = \langle (\hat{I}^\alpha - I^\alpha)(\hat{I}_\alpha - I_\alpha) \rangle \qquad (3)$$

where the expectation value is taken over all possible input ψ_α and detector χ_α noises. The noise-free part of the input I_α is, of course, deterministic, but since the snake does not "know" beforehand what the heat distribution looks like, we treat the input itself as a stochastic variable from a reconstruction point of view. If real input, i.e., a *specific realization* of some stochastic process, is presented to the sensory system, our model reconstructs an *optimal* input configuration for a given sensory response S_α. To this end we minimize the error (3) with respect to the coefficients of the reconstruction tensor ($\delta E_q / \delta R_\mu{}^\nu = 0$). In doing so, we encounter expectation values of correlations between the two different noise terms (ψ and χ) and the pure input

I, which we must specify. We take all cross correlations to be zero (the noise terms are independent of each other and the input strength) and autocorrelations to be given by

$$\langle \chi_\alpha \chi_\beta \rangle = \sigma_\chi^2 \delta_{\alpha\beta}, \qquad \langle \psi_\alpha \psi_\beta \rangle = \sigma_\psi^2 \delta_{\alpha\beta},$$
$$\langle I_\alpha I_\beta \rangle = \sigma_I^2 \delta_{\alpha\beta}, \qquad (4)$$

with $\delta_{\alpha\beta}$ as Kronecker delta. The first two equalities define the autocorrelation of the noise terms. Noise at different positions on the input or receptor manifold is taken to be independent with standard deviation $\sigma_{\chi/\psi}$. Input noise may be caused by small movements of prey animals, or by environmental disturbances such as vegetation moving in the wind. Detector noise may originate from physiological processes in the heat-sensitive cells in the pit membrane.

The third equality in (4) describes the autocorrelation of the input signal. We assume the correlation $\langle I_\alpha I_\beta \rangle$ of the input at different points $\alpha \neq \beta$ in space vanishes. Knowing the value of the input at one particular point does not tell us anything about its value at other points. In reality, this assumption will not hold. Neighboring points in space tend to have heat intensities that are alike since neighboring points will often be part of the same object and thus have nearly equal temperatures. Assuming the input correlations as in (4) to be independent makes reconstructing the input more difficult, since a potential source of information for the reconstruction (correlation in the input signal) is disregarded.

Minimizing (3) and using the correlations (4) and the definitions for the dimensionless parameters $\sigma := \sigma_\chi / \sigma_I$, $\tau := \sigma_\psi / \sigma_I$, we find for the components of the reconstruction tensor the following:

$$R^\mu{}_\gamma [T_\nu{}^\delta T^\gamma{}_\delta (1 + \tau^2) + \sigma^2 \delta_\nu^\gamma] = T_\nu{}^\mu. \qquad (5)$$

We note that τ, the noise-to-signal ratio of the input, will generally be small. Since it relates noise on the membrane, where input from many directions converges, to mean input intensity, σ need *not* be small. Solving (5) for $R_\alpha{}^\beta$ and using (2), we have a reconstruction of the original heat panorama with *only* the measured intensity on the membrane as input. The values of σ and τ can still be adjusted to get an optimal reconstruction. For the snake it is probably impossible to dynamically tune σ and τ to get the best reconstruction, but they may be determined to correspond to typical inputs and thereby give good results for most heat configurations the system encounters.

From (5) we see that the presence of noise in the input has no large effect on the value of the components of the reconstruction tensor. Since $\tau \ll 1$, we can effectively ignore the input noise in (5). The value of σ, however, *does* influence the reconstruction tensor. Because of the large organ aperture, every membrane point receives input from many input points. Conversely, information from one membrane point influences many pixels of the reconstructed image. A small measurement error may therefore have a large impact on the reconstruction.

We now turn to the transfer function $T_\alpha{}^\beta$, a geometrically determined quantity. A typical prey, such as a mouse or a rabbit, has a surface temperature of about 300 K. According to the Planck radiation law as an approximation of the emitted heat intensity, 99% of the radiation is emitted at wavelengths under 75 μm and the radiation intensity is maximal at $\lambda \approx 9.5$ μm, which is within the 8–12 μm ir atmospheric transmittance window [9]. Here the wavelength is much smaller than the organ aperture, such that we can use geometrical optics and ignore bending and refraction of the light rays. If the radiation intensity hitting the membrane at some point is larger than the emitted thermal radiation of the membrane itself, the membrane heats up at that location. In the converse situation, the membrane cools down locally.

The tensor $T_\alpha{}^\beta$ determines how effectively a heat source at position α outside the snake can heat up a pixel β on the pit membrane. We find

$$T_\alpha{}^\beta = \begin{cases} \mathbf{r}_{\alpha\beta}^{-2} \cos\phi_{\alpha\beta} & \text{if } \alpha \text{ is visible from } \beta, \\ 0 & \text{otherwise.} \end{cases} \quad (6)$$

Here $\mathbf{r}_{\alpha\beta}$ is the distance between the world point α and the membrane point β, and $\phi_{\alpha\beta}$ is the angle of incidence of the radiation on the membrane. If there is no line-of-sight between the points α and β (the pit organ boundary may be in the way) there is no heat transfer and $T_\alpha{}^\beta = 0$. For a circular input source the membrane heat distribution can be calculated analytically, as was first done by de Cock Buning [10]. Our approach generalizes his calculations to cope with arbitrary input and aperture.

To illustrate the abilities of our model, we presented the pit organ with a discretized version of Albrecht Dürer's famous hare; see Fig. 2. In the next step, we calculated the heat distribution on the membrane using the transfer function (6). Opinions on the exact dimensions of the pit organ and the number of heat receptors differ [1]. We have chosen conservative but realistic values that combine a relatively wide organ aperture and a moderate number of heat receptors. The calculated heat distribution on the membrane is shown in Fig. 3 (left).

Application of the reconstruction algorithm to the membrane image results in Fig. 3 (right). The quality improve-
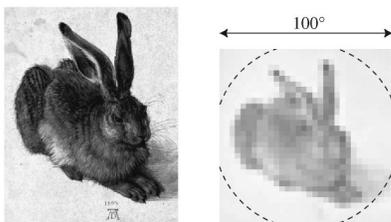
ment is spectacular, provided there is not too much detector noise. The information needed to reconstruct the heat panorama is still present in the membrane image (Fig. 3, left). This illustration is not biologically realistic; the object is far too large and the distributed gray levels do not correspond to a realistic thermal profile. This does not influence the performance of the algorithm, however, which would work just as well if the input object is nearly a point source, such as the warmth produced by the eyes of mammals relative to their body surface and surroundings.

The model has a fairly high noise tolerance. For input noise levels up to 50%, the hare is recognizable. Sensitivity to measurement errors is larger. In our calculations, one pixel of the reconstructed image corresponds to about 3°. For detector noise levels up to about 1% of the membrane heat intensity, a good reconstruction is possible, meaning that the edge of the hare may be determined with about one pixel accuracy. At detector noise levels beyond about 1%, the image is not so easily recognizable, but the presence of an object is still evident.

If the input is not very complicated (say, a small warm animal in front of a cold background) reconstruction may still be possible at higher detector noise levels. The low noise tolerance of the detection process results from the large impact of σ in (5) as discussed above. That is, the snake *does need* accurate detectors to get a reasonable reconstruction quality. Indeed, the experimentally determined membrane precision is high (1 mK) [2,3].

Changing the shape of the pit organ produces different characteristics. A narrow and deep organ has a much
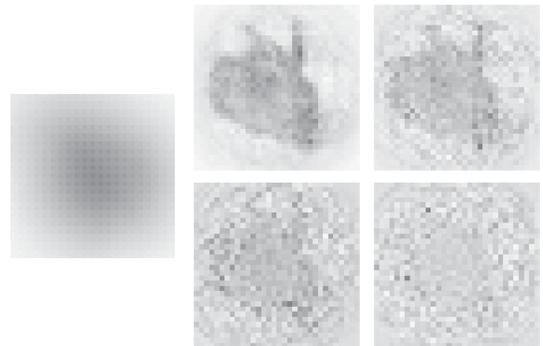

FIG. 3. On the left, this figure displays the membrane heat intensity as captured by the "pithole camera". On the right are reconstructions for four different membrane noise levels. Image quality of the reconstruction is spectacularly enhanced if little noise is present. The pit membrane was taken as a flat square containing 41×41 receptors. The model works equally well if applied to other membrane shapes. The membrane noise term χ_α was taken to be Gaussian with $\sigma_\chi = 25$, 100, 200, and 500 from left to right and top to bottom, corresponding to 0.25%, 1%, 2%, and 5% of the maximal membrane intensity. As input noise we took a Gaussian distribution with $\sigma_\psi = 10$, amounting to 10% of the input. Further parameter values are organ aperture (circular shape) = 0.8 mm, organ depth = 0.8 mm, membrane size = 1.2×1.2 mm, $\sigma = 0.8$, and $\tau = 0.1$.

FIG. 2. The famous hare by Dürer (left) was converted into 8-bit gray levels at a resolution of 32×32 (right). The result was presented to a pit organ at a distance of 1 m, its range [3], so as to fill the view field (dashed line, corresponding to 100°) of the organ.
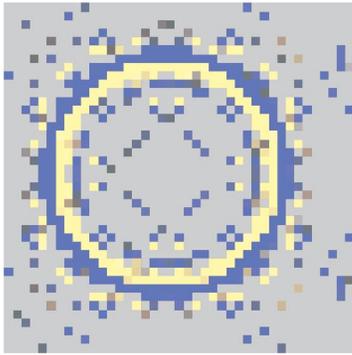
FIG. 4 (color online). Receptive field of a map neuron showing a ringlike structure. The excitatory (light/yellow) and inhibitory (dark/purple) input from the membrane receptors "filters" the membrane response so as to find the position the map neuron encodes.

better resolution than a wide and shallow one, but both view field and sensitivity will be limited. There is always a compromise between image quality and sensitivity. de Cock Buning [11] has suggested that in boids, such as pythons, a variety of differently formed pit organs exists, each adapted to a specific biological function.

A neuronal implementation of the model is fairly straightforward. The tensor $R_\alpha{}^\beta$ would correspond to a network of synaptic connections between the membrane ir detectors and neurons building a map in, for instance, the *optic tectum*. The strength of the individual connections would just be the value of the corresponding entry in $R_\alpha{}^\beta$, based on a rate coding [12]. Optimization of the coefficients (i.e., the synaptic strengths) can be obtained by comparing the information from the ir system with the visual map in the *optic tectum*, thus learning the proper synaptic strengths, e.g., through supervised spike-timing-dependent plasticity [13].

The neurons in the topological map receive excitatory (positive) as well as inhibitory (negative) input from the membrane receptors. The spatial distribution of these excitatory and inhibitory regions on the membrane (the *receptive field* of a neuron) in our model is shown in Fig. 4. Ringlike structures arise that detect the edges of projected images corresponding to the position that the map neuron encodes. A similar system (called *lateral inhibition*) is found in mammalian neurons receiving input from the retina [14], although the excitation-inhibition pattern there is disc-shaped rather than ringlike.

Hartline *et al.* [6] have found that the visual map and the ir map in the *optic tectum* are not aligned properly. They speculate that inhibitory interaction between the neurons might be diminished during anesthesia, and this may well have been the case [15]. If we repeat our model calculations with slightly diminished inhibitory components of $R_\alpha{}^\beta$, the neuronal reconstruction map shifts away from its normal position in such a way as to explain the offset found by Hartline *et al.* [6] This finding suggests that our model

contains at least the essential characteristics of neuronal ir processing.

Ultimately, a snake's ability to utilize information from the pit organs depends on its capability to detect edges in the image produced on the pit membrane. If the snake performed no reconstruction, but instead simply targeted bloblike "hot spots" on the membrane, it would still have to be able to discern the edge of the blob. The present model performs edge detection for all spatial positions and hence *automatically* creates a full reconstruction. A level of neuronal processing beyond what is represented in our model is unlikely to be beneficial since the quality of the system is fundamentally limited by the relatively small number of heat receptors.

In summary, it is possible to reconstruct the heat input to a snake's infrared-sensitive pit organ by only using the blurred heat distribution image from the pit membrane. The organ's large aperture does not prohibit formation of a clear neuronal image of the spatial heat distribution, but resolution is limited by the small number of heat receptors. This limitation agrees well with the reported accuracy of snake ir vision.

[1] G. J. Molenaar, in *Sensorimotor Integration*, edited by C. Gans and P. S. Ulinski, Biology of the Reptilia Vol. 17 (University of Chicago, Chicago, 1992), p. 367.
[2] T. H. Bullock and F. P. J. Diecke, J. Physiol. **134**, 47 (1956).
[3] J. Ebert and G. Westhoff, J. Comp. Physiol. A (to be published).
[4] J. L. van Hemmen, Chem. Phys. Chem. **3**, 291 (2002).
[5] E. A. Newman and P. H. Hartline, Sci. Am. **246**, No. 3, 98 (1982).
[6] P. H. Hartline, L. Kass, and M. S. Loop, Science **199**, 1225 (1978).
[7] E. A. Newman and P. H. Hartline, Science **213**, 789 (1981).
[8] R. C. Puetter, T. R. Gosnell, and Amos Yahil, Annu. Rev. Astron. Astrophys. **43**, 139 (2005).
[9] David A. Allen, *Infrared: The New Astronomy* (Wiley, New York, 1975).
[10] T. de Cock Buning, J. Theor. Biol. **111**, 509 (1984).
[11] T. de Cock Buning, Acta Biotheoretica **34**, 193 (1985).
[12] J.-M. P. Franosch, M. Sobotka, A. Elepfandt, and J. L. van Hemmen, Phys. Rev. Lett. **91**, 158101 (2003).
[13] J.-M. P. Franosch, M. Lingenheil, and J. L. van Hemmen, Phys. Rev. Lett. **95**, 078106 (2005).
[14] P. Buser and M. Imbert, *Vision* (MIT Press, Cambridge, MA, 1992), p. 296.
[15] H. G. Kress *et al.*, Anesthesiology **74**, 309 (1991).